

PACS numbers: 61.72. –y; 61.80.Ba; 61.80.Fe
DOI: 10.1070/QE2008v038n03ABEH013555

Individual induced absorption bands in MgF_2

A.P. Sergeev, P.B. Sergeev

***Abstract*. The absorption spectra of MgF_2 samples exposed to an electron beam and laser radiation at 248, 308, and 372 nm are investigated. Fourteen individual absorption bands are separated in the spectra. The parameters of the eight spectra of them are obtained for the first time. The separated bands are assigned to the intrinsic defects of the MgF_2 crystal.**

Keywords: *MgF_2, absorption bands, defects, ionising radiation, laser radiation.*

1. Introduction

The MgF_2 crystals are transparent for radiation at wavelengths above 110 nm and have a high mechanical strength. This makes them indispensable for operation with VUV radiation, in particular, with laser radiation. However, the MgF_2 windows exposed to short-wavelength radiation lose the transparency with time [1 – 6]. This also occurs under the action of other ionising radiations [7 – 16]. It was shown in papers [7 – 16] that upon irradiation of MgF_2 samples by the electron-beam, X-ray, gamma, and neutron pulses, as well as upon implantation of heavy ions, the absorption bands of MgF_2 monotonically increase. In this respect MgF_2 strongly differs from CaF_2 and BaF_2 crystals [10, 11, 13 – 15], which has not been explained so far.

The ionising radiation-induced absorption in MgF_2 negatively affects the efficiency of the windows of light sources. However, crystals with colour centres responsible for these absorption bands can be used for lasing, as optical filters, photochromic materials or some other applications. This requires the study of the properties of intrinsic colour centres in MgF_2.

In recent years we tested the radiation resistance of various optical materials for windows of excimer lasers by exposing these materials to electron beams [13 – 18]. The MgF_2 samples of different purities were also investigated [13 – 18]. A great number of the transmission spectra of the MgF_2 samples with electron-beam-induced absorption bands of different intensities were accumulated during these tests. These spectra in the range from 110 to 1000 nm were represented in the form of numerical tables $T(\lambda)$ and introduced to a PC, which considerably simplified their analysis.

After exposing to an electron beam, samples were stored in the dark at room temperature. Under such conditions, the relaxation of induced absorption is almost absent [7 – 9, 13 – 15]. Some of these samples were tested for the influence of light, in particular, laser radiation on the residual absorption in them. We obtained in this way a set of spectra characterising processes of the photoinduced formation of defects.

The aim of this paper is to reveal and systematise the individual absorption bands of MgF_2 and assign them to the corresponding colour centres based on the analysis of our experimental data and results reported in the literature. This is the most important stage on the way to understand the physics of defect formation processes in MgF_2 and the development of their models which are required for predicting the behaviour of crystals exposed to ionising and laser radiations.

2. Experimental

Our experimental studies of optical materials irradiated by electron beams were described in detail in many papers [13 – 18], and here we present only the most important details of the method.

The 3 – 5-mm-thick MgF_2 crystal samples of diameter ~ 12 mm were placed at our disposal by S.I. Vavilov State Optical Institute (SOI), Korth Kristalle and Corning Inc. (samples are denoted in the paper by the first letter S, K, or C of the manufacturer, respectively). According to certificates, the amount of impurities in samples from Korth Kristalle and Corning was ~ 20 ppm. The total content of impurities in samples from the State Optical Institute was an order of magnitude higher and the direction of optical axes in them was arbitrary. In all other samples, the [001] axis was perpendicular to the surface.

Samples were irradiated by an electron beam on the ELA setup [19]. They were placed in pits of a metal plate and covered by a titanium foil of thickness 14 – 80 μm. The thickness of the foil filter determined the energy of electrons incident on a sample and their pulsed energy fluence F_{el} [13 – 17]. Such an arrangement of samples minimises electric fields producing in dielectrics irradiated by charged particle beams [20]. In addition, the foil protected samples from illumination by light, in particular, by the luminescence of air excited by the electron beam.

A.P. Sergeev, P.B. Sergeev P.N. Lebedev Physics Institute, Russian Academy of Sciences, Leninsky prosp. 53, 119991 Moscow, Russia; e-mail: psergeev@sci.lebedev.ru

Received 2 March 2007; revision received 24 April 2007
Kvantovaya Elektronika **38** (3) 251 – 257 (2008)
Translated by M.N. Sapozhnikov

The electron beam used in experiments had the following parameters: the fluence was $F_{e1} \leqslant 2.4$ J cm^{-2}, the electron energy did not exceed 280 keV, the pulse duration was 80 ns, and the pulse repetition rate was about 20 pulses per hour. The total irradiation fluence F_e was determined as the sum of fluences of all pulses.

After irradiation of samples with the required fluence F_e, their transmission spectra $T(\lambda)$ were measured in the visible region with a Genesis-2 Spectronics spectrophotometer and with a BMP-2 spectrophotometer in the region from 120 to 240 nm. These spectra were represented in the form of numerical tables with a wavelength step equal, as a rule, to 3 nm. Typical transmission spectra of MgF_2 samples irradiated by the electron beam with different fluences F_e are presented in Fig. 1 (digits after the sign _ in J cm^{-2}).

The optical density spectra $D(\lambda)$ were obtained by the point-by-point transformation of the transmission spectra by using the expression

$$D(\lambda) = \ln\left[\frac{T_0(\lambda)}{T(\lambda)}\right], \quad (1)$$

where T_0 is the initial transmission of the sample. Figure 2 shows typical spectra $D(\lambda)$ corresponding to spectra $T(\lambda)$ in Fig. 1.

The main part of samples was irradiated by the electron beam with the total fluence up to 3–4 kJ cm^{-2}, and for a pair of samples from the SOI the fluence achieved 10 kJ cm^{-2}. In the latter case, the dose absorbed in the near the surface region of thickness ~ 0.1 mm was about 3×10^8 Gy. Such an irradiation level was higher than that achieved earlier in most cases [7–11], which allowed us to find some new features in the induced absorption spectra of MgF_2, in particular, a band at 465 nm, which is observed in Fig. 1 for a sample from the SOI for $F_e \sim 10$ kJ cm^{-2}, and also a band at 517 nm.

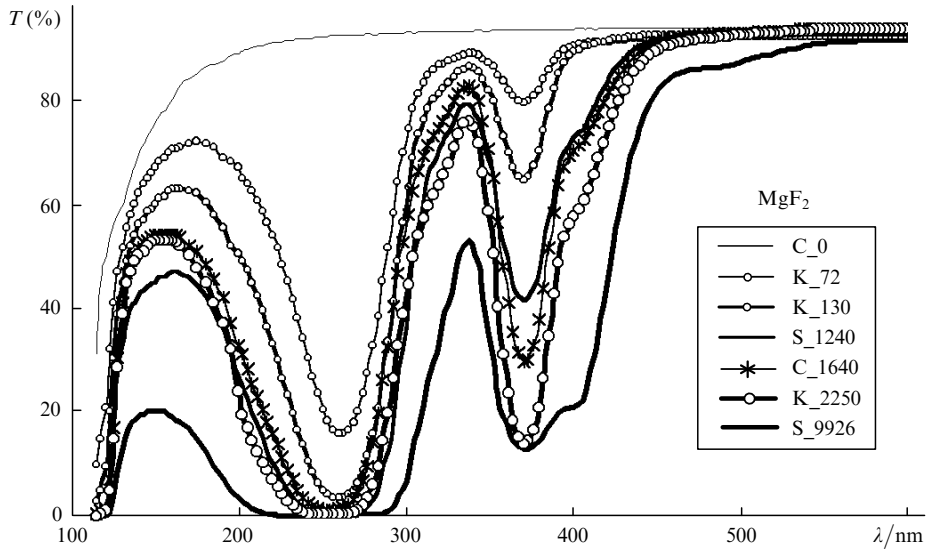

Figure 1. Typical transmission spectra of MgF_2 samples from different manufacturers after irradiation by an electron beam with the fluence F_e (manufacturer _ F_e in J cm^{-2}).

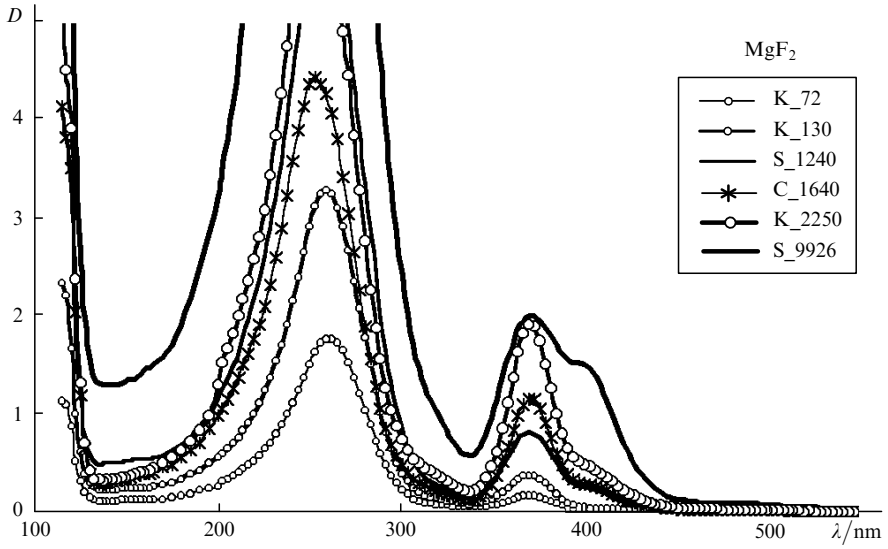

Figure 2. Optical density spectra corresponding to the transmission spectra of MgF_2 samles in Fig. 1.

3. Individual bands in the absorption spectra of MgF_2

With a great number of induced absorption spectra of MgF_2 of different intensities at our disposal, we could apply the Alentsev–Fock method [21] and difference methods to separate individual absorption bands. We also used the results of papers [1–12, 22–24], in which the characteristics of a number of bands in the spectral region between 200 and 500 nm have been already determined and the bands themselves have been assigned to the corresponding colour centres. The first results of these studies were discussed in [15, 25]. Here we present in detail all the data refined recently.

We found that most of the individual absorption bands of MgF_2 were well described by a Gaussian profile over the energy E:

$$A_N = K_N \exp\{-\ln 2[(E_N^{\max} - E)/\Delta E_N]^2\}. \quad (2)$$

If the wavelength λ is used instead of the energy E, expression (2) takes the form

$$A_N = K_N \exp\{-\ln 2[(\lambda_N^{\max} + \Delta\lambda_N)/\Delta\lambda_N]^2 \times [(\lambda_N^{\max} - \lambda)/\lambda]^2\}. \quad (3)$$

Here, $E_N^{\max}$ and $\lambda_N^{\max}$ are the positions of the maximum of the N-th absorption band in the energy and wavelength scales; ΔE_N and $\Delta\lambda_N$ are the half-widths of the N-th absorption band in these scales; and K_N is the amplitude coefficient of the band. The shape of some bands was more accurately described by the expression

$$A_N = K_N \exp\{-\ln 2[(\lambda_N^{\max} - \lambda)/\Delta\lambda_N]^2\}. \quad (4)$$

Expressions (3) and (4) were used to describe the individual absorption bands being separated. This considerably simplified the calculations performed in the decomposition of a great number of experimental spectra into individual components.

The parameters of all the separated bands corresponding to the Gaussian approximation by expressions (3) and (4) are presented in Table 1. The bands described by expression (4) are indicated in the first column by the asterisk. The values of $\lambda_N^{\max}$ and $\Delta\lambda_N$ for all the bands were determined with accuracies of 3 nm and 10 %, respectively.

Table 1. Parameters of individual absorption bands of MgF_2.

N	$\lambda_N^{\max}$/nm	$E_N^{\max}$/eV	$\Delta\lambda_N$/nm	K_N
1	117	10.7	5	4.5
2	140	8.9	17	0.33
3	170	7.3	16	0.35
4	202	6.2	22	0.33
5	217	5.7	33	1.35
6	250	5.0	28	3.53
7	259	4.8	17	2.63
8	276	4.5	12	0.01
9*	300	4.2	13	0.01
10	320	3.9	20	0.22
11*	370	3.37	13	1.85
12	400	3.1	23	0.42
13	465	2.7	33	0.02
14	517	2.4	35	0

We have managed to fit the shape of all experimental spectra $D(\lambda)$ by summing individual spectral bands with the properly selected amplitude coefficients K_N. Figure 3 presents the results of one of such reconstructions performed for a K_2250 sample (Korth Kristallke sample irradiated by an electron beam with the fluence 2250 J cm^{-2}). The curves denoted by L$\lambda_N^{\max}$ are individual absorption bands. The amplitude coefficients used in this case are presented in Table 1. They characterise the relative contribution of the individual components to the induced absorption spectrum of MgF_2. The coefficients K_N were determined with an accuracy of ~ 10 % for $K_N > 1$, ~ 30 % for $K_N \sim 0.1$ and more than 100 % for $K_N \lesssim 0.01$. Note that the parameters of the bands with $K_N \sim 0 - 0.02$ presented in Table 1 were found and refined from the spectra of other samples, where these bands were much stronger. Note also that the parameters of the bands 1–5, 8, 13, 14 are presented for the first time, although some of them are mentioned in the literature, which will be discussed below.

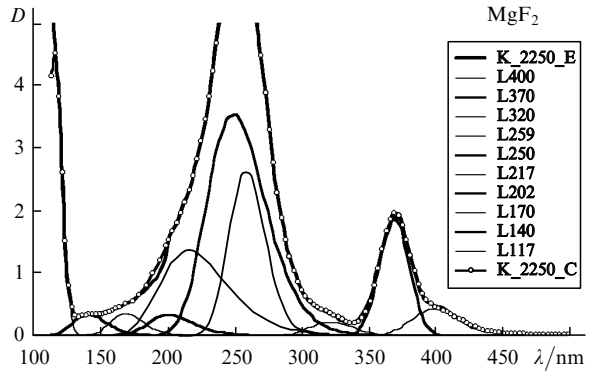

Figure 3. Decomposition of the optical density spectrum of the K_2250 sample (a Korth Kristalle sample irradiated by an electron beam with the fluence 2250 J cm^{-2}) into individual bands Lλ. K_2250_E is the experimental spectrum; K_2250_C is the spectrum calculated taking into account the contributions of all individual bands. Weak bands with $K_N < 0.1$ are not shown.

4. Phototransformation of the absorption spectra of MgF_2

The selective excitation of MgF_2 into its absorption bands leads to a change in the band intensity, as in the case of many other crystals. This effect has long been used to study the nature of colour centres in MgF_2 [1–5, 7–10]. The separation of individual bands in the absorption spectrum of this crystal allows us to describe this effect quantitatively, which will be demonstrated in this section.

The excitation of a MgF_2 crystal into the absorption band of F-centres (a strong band at 260 nm in Figs 1 and 2) leads to a strong bleaching in this band [7–10]. The absorption bands corresponding to other colour centres also change. We observed these effects by using a 248-nm KrF laser in the ELA setup [19]. The laser radiation fluence in a 80-ns pulse on samples was 0.1 J cm^{-2}. Radiation fluences in the first, second, and third pulse series were 5, 6, and 25 J cm^{-2}, and the total fluence after each successive series was 5, 11, and 36 J cm^{-2}, respectively. The absorption spectra of samples were recorded after each irradiation.

Figure 4 presents the spectra $D(\lambda)$ of one of the Corning MgF_2 samples (C1) irradiated by an electron beam with

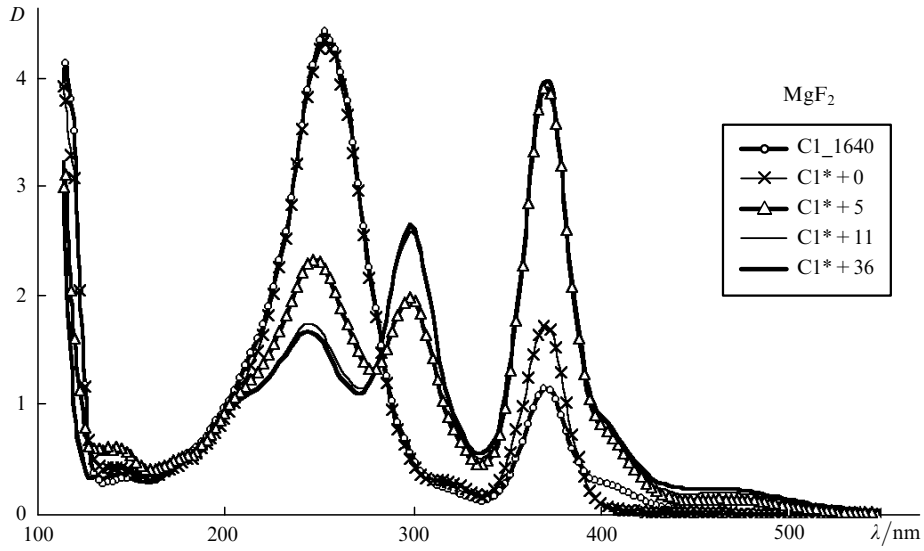

Figure 4. Optical density spectra of the C1 sample irradiated by an electron beam with $F_e = 1640$ J cm^{-2} after two-year storage before irradiation by the KrF laser (C1* + 0) and after irradiation with the total fluence 5 (C1* + 5), 11 (C1* + 11), and 36 J cm^{-2} (C1* + 36).

$F_e = 1640$ J cm^{-2}, which was kept in the dark before laser irradiation for two years (curve C1* + 0). Curves C1* + 5, C1* + 11, and C1* + 36 are the spectra of the same sample irradiated by series of KrF laser pulses (figures after the sign '+' correspond to the total fluence in J cm^{-2}).

One can see from Fig. 4 that after the first series of laser pulses, the 260-nm absorption band very strongly decreases, whereas all the longer-wavelength absorption bands increase. As the crystal is further irradiated by the KrF laser, the 260-nm band further decreases, while the 300-nm band noticeably increases.

This behaviour of the absorption bands is manifested in the change in coefficients K_N, which are presented in the third–seven columns in Table 2. The coefficients in the third and fourth columns characterise the relaxation of the absorption bands during the storage of the sample in the dark at room temperature for two years. The values of K_N presented in the fourth–seven columns characterise the band intensities before and after irradiation of the sample by the KrF laser. The change in coefficients K_N reflects processes proceeding in the crystal.

Within five months after experiments with the KrF laser, sample C1 was irradiated by a 308-nm XeCl laser. The total fluence for 200 75-ns pulses was 16 J cm^{-2}. The optical density spectrum of sample C1 before irradiation (C1** + 0) virtually coincided with the C1* + 36 spectrum. This spectrum and the (C1** + 16*) spectrum of sample C1 recorded after irradiation by the XeCl laser are presented in Fig. 5. The changes observed in the spectra can be readily explained by comparing the values of coefficients K_N in the seven and eight columns of Table 2. In the given case, the intensity of the 300-nm and 465-nm bands decreased by a factor of 2.4, whereas the 217-nm band intensity approximately doubled and the 517-nm band intensity increased by a factor of 1.5.

After all the laser irradiation experiments, sample C1 was again irradiated by the electron beam on the ELA setup. The additional electron-beam fluence increased after six pulses up to 10 J cm^{-2}. The absorption spectrum of the sample obtained after such irradiation is shown in Fig. 5 (C1***_10). One can see that this spectrum virtually coincides in many regions with the initial C1_1640 spectrum. The degree of this coincidence for all the bands can be quantitatively estimated by comparing the corresponding coefficients in the third and last columns of Table 2.

Except experiments with KrF and XeCl lasers, we also

Table 2. Coefficients K_N for the corresponding absorption spectra of the C1 MgF_2 sample.

N	λ_N^{max}/nm	C1_1640	C1* + 0	C1* + 5	C1* + 11	C1* + 36	C1** + 16*	C1***_10
1	117	4	4	2	1.8	1.8	2.2	3.2
2	140	0.29	0.4	0.6	0.35	0.35	0.47	0.4
3	170	0.35	0.3	0.3	0.27	0.24	0.3	0.3
4	202	0.38	0.27	0.5	0.41	0.56	0.41	0.25
5	217	0.75	0.8	0.58	0.6	0.44	0.9	1
6	250	2.7	2.5	1.85	1.3	1.35	1.4	2.05
7	259	1.5	1.6	0.15	0.1	0	0	2.5
8	276	0	0	0.02	0.15	0.09	0.07	0.27
9*	300	0.01	0	1.49	2.1	2.2	0.92	0.1
10	320	0.1	0.18	0.55	0.7	0.7	0.83	0.1
11*	370	1.1	1.7	3.85	3.62	3.9	3.91	0.4
12	400	0.23	0.01	0.7	0.71	0.8	0.75	0.2
13	465	0.02	0	0.13	0.19	0.23	0.09	0.008
14	517	0	0	0.01	0.015	0.033	0.048	0

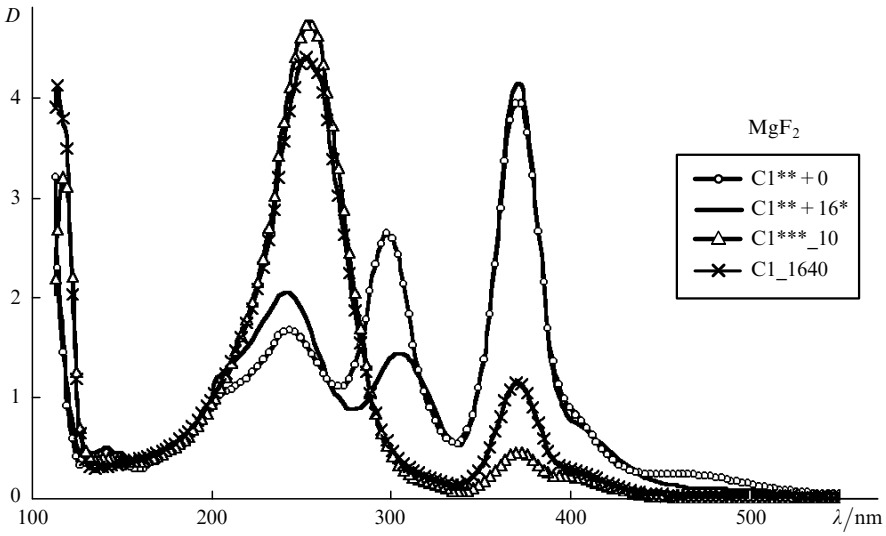

Figure 5. Optical density spectra of the C1 sample before (C1** + 0) and after irradiation by the XeCl laser (C1* + 0) with the total fluence 16 J cm^{-2} (C1** + 16*) and the initial spectrum after irradiation of the sample by an electron beam with $F_e = 1640$ J cm^{-2} (Cl_1640) and its additional irradiation with $F_e = 10$ J cm^{-2} (C1***_10).

studied the stability of another strong absorption band at 370 nm with respect to selective laser excitation. We used in these experiments the 372-nm second harmonic of a Ti : sapphire laser. The fluence of a 50-fs pulse from this laser was ~ 2 mJ cm^{-2}. The pulse repetition rate was 10 Hz. Experiments were performed with a Korth Kristalle sample (K3), which was preliminarily irradiated by the electron beam with $F_e = 2680$ J cm^{-2}. The total fluence at 372 nm for a series of pulses was 10 J cm^{-2}.

Variations induced in the absorption spectra in these experiments were described earlier in [15]. Therefore, we again will characterise the transformation of the spectra only by the coefficients K_N, which are presented in Table 3. The third column K3 + 0 gives the values of K_N for the spectrum of sample K3 irradiated by the electron beam with $F_e = 2680$ J cm^{-2}, which was stored for two years before experiments with laser irradiation. The fourth, fifth, and sixth columns present K_N for spectra recorded within 3 min (*), 5 days (**), and 5 months (***) after laser irradiation of sample K3 at 372 nm with the total fluence of 10 J cm^{-2}.

One can see from the third and fourth columns in Table 3 that only bands 8–12 exhibit a noticeable photo-induced transformation. After laser irradiation at 372, the 370-nm absorption band intensity decreases almost by an order of magnitude. The 320-nm band intensity decreases by three times. In this case, the intensity of the 400-nm band increases almost by three times, while the intensity of the 279-nm and 465-nm bands doubles. One can see from the two last columns that after laser irradiation bands 10–12 relax to the initial state, whereas bands 13 and 14 almost do not change.

We also studied the behaviour of the electron-beam induced absorption in MgF_2 irradiated by a mercury lamp. These experiments were performed with SOI samples irradiated by electron beams with fluences ~ 100 and 1000 J cm^{-2}. Samples were placed at a distance of 6 cm from the discharge tube of a RGD-2 mercury lamp and were irradiated for a certain time. The absorption spectra of samples mainly coincided with those observed in [7, 9]. Therefore, we again describe the photoinduced transformation of spectra with the help of coefficients K_N. Table 4 presents the results of the study of sample S21 irradiated by the electron beam with $F_e = 1240$ J cm^{-2}, which was stored then in the dark for two years (S21* + 0), and the coefficients K_N for the absorption spectra of MgF_2 recorded after irradiation of the sample by the mercury sample for three (+3) and thirty (+30) minutes.

In these experiments, the intensity of the 259-nm and 276-nm bands strongly decreased, while the intensity of longer-wavelength bands increased. The behaviour of the

Table 3. Coefficients K_N for the corresponding absorption spectra of the K3 MgF_2 sample.

N	λ_N^{max}/nm	K3 + 0	K3 + 10*	K3 + 10**	K3 + 10***
4	202	0.6	0.7	0.7	0.7
5	217	1.3	1.3	1.3	1.3
6	250	4.1	4.3	4.3	4.3
7	259	3.3	3	3	3
8	279	0.38	0.7	0.7	0.7
9	300	0.01	0.04	0.04	0.04
10	320	0.34	0.12	0.14	0.18
11	370	2.04	0.285	0.53	1.03
12	400	0.18	0.56	0.478	0.47
13	465	0.005	0.009	0.014	0.013
14	517	0.007	0.005	0.008	0.008

Table 4. Coefficients K_N for the corresponding absorption spectra of the S21 MgF_2 sample.

N	λ_N^{max}/nm	Γ21* + 0	Γ21* + 3	Γ21* + 30
4	202	0.5	0.6	0.6
5	217	1.29	1.1	1.1
6	250	2.6	2.5	2.6
7	259	1.5	1.5	0.5
8	276	1.3	0.5	0.2
9	300	0.25	0.5	0.75
10	320	0.23	0.27	0.4
11	370	0.87	1.57	2.1
12	400	0.25	1.35	1.05
13	465	0.05	0.1	0.15
14	517	0.048	0.04	0.04

400-nm band was unusual. The intensity of this band after the first irradiation for three minutes even exceeded the 370-nm band intensity, but it decreased upon further irradiation. This was pointed out earlier in [8].

As the sample was further irradiated, the ratio of the band intensities formed after irradiation for 30 minutes almost did not change. Upon completion of experiments with the mercury lamp, the intensity of the 400-nm band of samples decreased, while the 370-nm band intensity increased, as for sample K3. Note also that bands 6–8 had substantially different photostabilities.

5. Discussion of the results

The separation of individual spectral bands in a complex absorption spectrum immediately poses the question of their origin. Based on the results presented above and taking into account the data reported in papers [1–12, 22–24] and the fundamentals of the physics of defect crystals [26, 27], we made the following conclusions.

The first absorption band at 117 ± 3 nm with the half-width 5 ± 1 nm undoubtedly belongs to α-centres. The position of this band at the UV boundary of the crystal transmission unambiguously specifies its nature [27]. The band intensity is high, as that of the F-centre bands, and monotonically increases with increasing the electron-beam fluence. Upon laser irradiation into the F band, the band intensity decreases synchronously with absorption by α-centres (see Table 2).

The second band at 140 nm belongs to I-centres. This band located near the bands of α-centres was observed in many other crystals [27]. Its intensity was very low even for high F_e, which suggests that the formation efficiency of I-centres is low. This band was observed most distinctly in experiments with the KrF laser (Fig. 4). The authors of paper [3] assigned it to surface colour centres.

The band at 170 nm has unusual properties. It is virtually insensitive to laser radiation at 248, 308, and 372 nm used in experiments and has almost the same intensity in different samples for the electron-beam fluence varied from ~ 1000 to 2000 J cm^{-2} (Fig. 2). All this confirm the conclusion that this band belongs to surface colour centres [3]. These can be also centres related to the impurity oxygen. According to [4], the presence of oxygen in a sample volume is manifested in absorption in the region 162–165 nm.

It has long been established that the bands at 250 and 259 nm belong to F-centres of different configurations, and light with different polarisations is absorbed in them differently [1–11]. These bands in real crystals merge to form the strongest absorption band of MgF_2 with the maximum in the range from 250 to 265 nm according to different studies [1–15]. The optical density D(256 nm) in our experiments achieved ~ 5 already for $F_e \sim 1$ kJ cm^{-2}. We could not measure the value of D at larger values of F_e by the method used in the study. For this reason, we measured the dependence of D on F_e at the band wing (at a wavelength of 301 nm) [16]. We found that the value of D(301 nm) almost linearly increased with increasing F_e up to ~ 10 kJ cm^{-2} in all samples under study. The slope of straight lines D(F_e) was smaller for purest samples. Similar dependences of the intensity of absorption bands of F-centres on the absorbed dose of different ionising radiations were observed earlier [7, 8, 10].

The ratio of the amplitude coefficients K_6/K_7 upon electron-beam irradiation of samples was ~ 1.8. After irradiation, this ratio increased for all samples with time mainly due to the decrease in the 259-nm band intensity. One can see from Tables 2 and 4 that laser excitation into this band leads to its rapid and almost complete disappearance. In this case, the intensity of all the longer-wavelength bands increases. The reason for such a drastic difference in the photosensitivity of the 250-nm and 259-nm bands of F-centres is not clear yet.

Experiments on bleaching of SOI MgF_2 samples by radiation from a mercury lamp revealed a new absorption band at 276 ± 3 nm. The photosensitivity of this band was even higher than that of the 259-nm band. This band was also found in the absorption spectra of other samples. However, its intensity in pure samples was considerably lower than in SOI samples. This suggests that the new band can be assigned to F-centres localised near impurity atoms [26, p. 59]. Such a domination impurity in SOI samples was oxygen. Note that the intensity of this band in pure samples irradiated by different sources also increased with time, which is demonstrated in Table 2. This can be caused by the radiation-induced diffusion of oxygen and other impurities to samples.

Note also that we have managed to simulate quite accurately the induced absorption spectra of MgF_2 after 'burning' the 259-nm and 279-m bands (Figs 4 and 5) by using basis bands from Table 1 and shifting the maximum of band 6 from 250 to 248 nm. It was unnecessary to introduce additional bands in the region between 245 and 24 nm, as has been done in [5, 10]. However, we found in simulations that the maxima of a number of bands should be shifted within 1–3 nm and their widths should be varied within ±10 % to fit experimental spectra by calculated spectra. Such shifts can be justified by concentration effects and the presence of various impurities. These parameters can also depend on temperature [8, 9, 22].

The strong absorption band at 370 nm belongs to M-centres (a pair of F-centres in adjacent lattice points) [1–12]. Absorption bands at 320 and 400 nm also belong to these centres [5, 8–10, 12]. The authors of paper [12] also assigned the 219-nm band to these centres. We assume that in our case this is the 217-nm band. Thus, we assign the four bands at 217, 320, 370, and 400 nm to M-centres. Note that the relative intensities of these bands are not constant. They strongly depend on many factors such as the purity samples, their irradiation regimes, the time after irradiation and storage conditions, and illumination regimes. This should be taken into account in studying the nature of M-centres and other colour centres in MgF_2.

Let us now discuss the behaviour of the shortest-wavelength band at 202 nm. After the first irradiation of sample C1 by the KrF laser, the concentration of F- and α-centres drastically decreases and the intensity of the main absorption band of M-centres at 370 nm approximately doubles. The intensity of the 202-nm band also increases. The intensity of this band changes then as that of the 370-nm band. All these variations in the intensity of the 202-nm band can be at least qualitatively explained by its belonging to the M^+-centre, i.e. a pair of adjacent F- and α-centres [26, p. 65]. Thus, we assign the 202-nm band to this intrinsic defect of MgF_2.

After the first series of pulses in experiments with sample C1 irradiated by the KrF laser, we found that the amplitude

coefficient K_9 of the 300-nm band drastically increased from zero to $\sim 1.5-2$. Absorption at 465 nm (K_{13}) also increased. In this case, the ratio K_9/K_{13} was constant within the measurement error and equal to 10. This suggests that these bands can be interrelated. To verify this assumption, we irradiated sample C1 by the XeCl laser at 308 nm. A comparison of the values of K_9 and K_{13} in the two next-to-last columns of Table 2 shows that these coefficients decreased after irradiation approximately by the same factor of 2.4. This indicates that the 300-nm and 465-nm bands can belong to the same absorbing centre. Among the intrinsic defects of MgF_2, this can be the H-centre. The maximum of the UV absorption band of this centre at 300 nm (4.2 eV) coincides with the value predicted in [22, 23]. The presence of the long-wavelength 465-nm band, which is inherent in the H-centre, also confirms this conclusion.

If our assumption is correct, the question arises about the reasons for such a strong behaviour of these Frenkel defects in MgF_2 during the production of other defects (F- and M-centres) by ionising radiations. Indeed, upon irradiation by an electron beam, the concentration of the F- and M-centres monotonically increases, whereas the concentration of H-centres remains very low. Then, after photoexcitation into the F-band, the concentration of H-centres (if bands 9 and 13 belong to them) drastically increases. The reason for such unusual behaviour of the 300-nm and 465-nm bands and centres related to them remains unclear.

The nature of the new 517-nm band is also uncertain yet due to the absence of information on its properties. This band can belong either to M^--centres or R-centres. To determine the nature of this band, both experimental and theoretical studies are required.

It should be emphasised that the absorption spectrum of MgF_2 transformed after photoexcitation can be almost completely recovered after irradiation of MgF_2 by an electron beam. This effect was observed earlier for the 370-nm band in [28]. We found that such a recovery was also observed for bands 4, 9 – 14. The nature of this effect is not clear yet, but it obviously can be used for many practical applications.

Although the nature of the basic induced-absorption bands in MgF_2 is not clear yet, their separation offers a new tool for the quantitative description and detailed study of formation of defects in MgF_2 crystals, which is of interest both for science and technology.

6. Conclusions

In this paper, we have separated electron-beam-induced absorption spectra in MgF_2 into 14 individual bands located in the region from 110 to 600 nm. The shape of each of the bands was described by a Gaussian with parameters (the wavelengths of the band maximum and the FWHM) presented in Table 1. The parameters of the eight of these bands have been obtained for the first time. By using the separated basic bands with appropriately selected amplitude coefficients, we have fitted all the induced absorption spectra observed in MgF_2 samples. This gives a new instrument for the quantitative description of radiation-induced formation of defects in a MgF_2 crystal by analysing variations in the amplitude coefficients of individual spectral bands, which was demonstrated in a number of experiments.

It has been found that all radiation-induced defects in MgF_2 are destructed after exposing MgF_2 to an electron beam. This is accompanied by the recovery of F-centres.

Acknowledgements. The authors thank D.B. Stavrovski and V.M. Reiterov for measuring the VUV absorption spectra of samples and useful advice and also V.M. Borisov and O.B. Khristoforov for irradiation samples by the XeCl laser.

References

1. Shishatskaya L.P. et al. *Opt.-mekh. Prom.*, (10), 69 (1972).
2. Shishatskaya L.P., Lisitsyn V.M. *Opt.-mekh. Prom.*, (8), 53 (1978).
3. Budina N.E., Reiterov V.M., Shishatskaya L.P. *Opt.-mekh. Prom.*, (9), 48 (1982).
4. Apinov A. et al. *Opt.-mekh. Prom.*, (8), 10 (1983).
5. Zhukova E.V. et al. *Opt. Zh.*, **69** (3), 25 (2002).
6. Hata K., Watanabe M., Watanabe S. *Appl. Phys. B*, **50**, 55 (1990).
7. Blunt R.F., Cohen M.I. *Phys. Rev.*, **153**, 1031 (1967).
8. Sibley W.A., Facey O.E. *Phys. Rev.,* **174**, 1076 (1968).
9. Facey O.E., Sibley W.A. *Phys. Rev.*, **186**, 926 (1969).
10. Nikanovich M.V. et al. *Opt. Spektrosk.*, **60**, 307 (1986).
11. Vakhidov Sh.A. et al. *Zh. Tekh. Fiz.*, **51**, 2325 (1981).
12. Davidson A.T. et al. *Phys. Rev. B,* **48**, 782 (1993).
13. Sergeev P.B. et al. *Proc. 12th Int. Conf. on Radiation Physics and Chemistry of Inorganic Materials* (Tomsk, Russia, 2003) p. 82.
14. Mironov I.A. et al. *Proc. SPIE Int. Soc. Opt. Eng.,* **5479**, 135 (2003).
15. Sergeev A.P., Sergeev P.B., Zvorykin V.D. *Izv. Vyssh. Uchebn. Zaved. Ser. Fiz.*, (10), 312 (2006).
16. Sergeev P.B. et al. *Opt. Zh.*, **72**, 493 (2005).
17. Sergeev P.B. et al. *Opt. Zh.*, **71**, 93 (2004).
18. Sergeev P.B., Sergeev A.P., Zvorykin V.D. *Kvantovaya Elektron.*, **37**, 706 (2007) [*Quantum Electron.,* **37**, 706 (2007)].
19. Sergeev P.B. *J. Sov. Laser Res.,* **14** (4), 237 (1993).
20. Boev S.G., Ushakov V.Ya. *Radiatsonnoe nakoplenie zaryada v tverdykh dielektrikakh i metody ego diagnostiki* (Radiative Accumulation of Charges in Solid Dielectrics and Methods of Its Diagnostics) (Moscow: Energoatomizdat, 1991) p. 12.
21. Fock M.V. *Trudy FIAN*, **59**, 3 (1972).
22. Williams R.T. et. al. *Phys. Rev. B*, **15**, 5003 (1977).
23. Song K.S., Williams R.T. *Self-Trapped Excitons* (Berlin, Heidelberg, New York: Springer-Verlag, 1993).
24. Lisitsyna L.A., Korepanov V.I., Grechkina T.V. *Spektrosk. Tverd. Tela*, **95**, 797 (2003).
25. Sergeev A.P. *Tezisy konf. 'Fundamental'nye i prikladnye problemy sovremennoi fiziki'* (Proceedings of Conference on Fundamental and Applied Problems of Modern Physics) (Moscow: FIAN, 2006) pp 226, 227.
26. Stoneham A.M. *Theory of Defects in Solids: the Electronic Structure of Defects in Insulators and Semiconductors* (Oxford: Clarendon Press, 1975; Moscow: Mir, 1979) Vol. 2.
27. Lushchik Ch.B., Lushchik A.Ch. *Raspad elektronnykh vozbuzhdenii s obrazovaniem defektov v tverdykh telakh* (Decay of Electronic Excitations with the Formation of Defects in Solids (Moscow: Nauka, 1985) p. 101.
28. Baryshnikov V.I. et al. *Opt. Spektrosk.*, **67**, 217 (1989).